

See discussions, stats, and author profiles for this publication at: <https://www.researchgate.net/publication/236931872>

# Conformational Study of GSH and GSSG Using Constant-pH Molecular Dynamics Simulations

ARTICLE *in* THE JOURNAL OF PHYSICAL CHEMISTRY B · MAY 2013

Impact Factor: 3.3 · DOI: 10.1021/jp401066v · Source: PubMed

---

CITATIONS

10

---

READS

44

## 4 AUTHORS:



[Diogo Vila-Vicosa](#)

University of Lisbon

17 PUBLICATIONS 72 CITATIONS

[SEE PROFILE](#)



[Hugo A F Santos](#)

University of Lisbon

4 PUBLICATIONS 13 CITATIONS

[SEE PROFILE](#)



[Vitor H Teixeira](#)

University of Lisbon

23 PUBLICATIONS 521 CITATIONS

[SEE PROFILE](#)



[Miguel Machuqueiro](#)

University of Lisbon

36 PUBLICATIONS 704 CITATIONS

[SEE PROFILE](#)

# Conformational Study of GSH and GSSG Using Constant-pH Molecular Dynamics Simulations

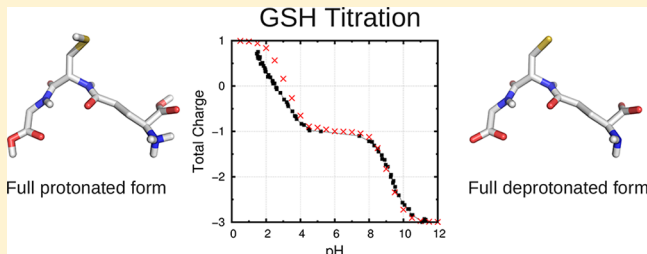
Diogo Vila-Viçosa, Vitor H. Teixeira, Hugo A. F. Santos, and Miguel Machuqueiro\*

Centro de Química e Bioquímica and Departamento de Química e Bioquímica, Faculdade de Ciências, Universidade de Lisboa, 1749-016 Lisboa, Portugal

Supporting Information

**ABSTRACT:** Glutathione is a small peptide with a crucial role in living organisms. This molecule is found in Nature in both reduced (GSH) and oxidized (GSSG) forms and a high GSH/GSSG ratio is essential to the cell. Glutathione is also present in several enzymatic reactions and can be found in many protein structures. As small peptides, these molecules do not have a defined structure in solution and are able to sample a broad conformational space. In addition, both molecules have several titration sites (four in GSH and six in GSSG) and their conformational space is inevitably influenced by pH.

Here, we present a detailed conformational study of GSH and GSSG in a range of pH values, together with a full pH titration of these molecules. We performed constant-pH MD simulations of GSH and GSSG at 24 pH values in a total of 14.4  $\mu$ s (300 ns per pH value). We obtained the two titration curves and the  $pK_a$  values for all titratable groups with good agreement with experimental data. We also observed that GSH and GSSG have a large conformational variability in solution and their structural preferences are not significantly affected upon binding to proteins. Some exceptions were found and investigated in detail.



## INTRODUCTION

Glutathione is a special water-soluble peptide with a crucial role in living organisms, being involved in different reactions catalyzed by a myriad of enzymes. This tripeptide can be found in oxidized disulfide (GSSG) or reduced thiol (GSH) states (Figure 1). Glutathione is used *in vivo* almost exclusively in the reduced state, hence the importance of a high GSH/GSSG ratio in the cell.<sup>1</sup> The maintenance of the optimal ratio is tightly regulated with the help of a class of enzymes called glutathione reductases (GSR).<sup>1</sup> A lower ratio in the cytosol may be indicative of oxidative stress or cellular toxicity.<sup>2,3</sup> The thiol group in GSH renders it a potent reducing agent and allows an important role in the detoxification of various electrophilic compounds and peroxides as a cofactor of glutathione-S-transferases (GST) and glutathione peroxidases (GPx). Other minor classes like thioredoxin-reductases, thioredoxins, and protein-disulfide isomerases also interact with GSH.<sup>3</sup>

The structure of GSH has been determined by both NMR spectroscopy and X-ray crystallography isolated<sup>4–6</sup> and bound to different proteins.<sup>7–62</sup> Also, there are several computational studies addressing GSH conformational preferences using molecular mechanics and quantum mechanics methodologies.<sup>63–72</sup> As most small peptides, GSH does not present a specific structure in solution, but rather an ensemble of conformations which vary according to different factors like protein and membrane interactions, or pH.<sup>67</sup> In fact, due to its 4 titratable sites, the reduced GSH conformational space should be significantly affected by the solution pH. The  $pK_a$  values of GSH have been determined by several authors using NMR

spectroscopy<sup>73–76</sup> or potentiometry.<sup>76,77</sup> NMR data was also used to infer on the conformational preferences of the tripeptide.<sup>66,74,78</sup> More recently, several authors have been trying to model GSH conformational space using molecular dynamics (MD)<sup>67–70</sup> and/or first principles methods.<sup>63–66,71,72</sup> One of the most extensive conformational analyses of GSH in water using MD was done by Rauk and co-workers.<sup>67</sup> Unfortunately, these authors were not able to explicitly introduce pH in their simulations. Alternatively, they simulated all possible pure charge states and compared the structures and energies of the most stable conformations obtained. This approach is limited because it neglects the coupling between protonation and conformation.

MD simulations deal with pH in a rather limited way, usually by setting the protonable groups of the molecules to the states they would have in solution at the intended pH. On the other hand, more simplified approaches, like those based on Poisson–Boltzmann (PB) and Monte Carlo (MC) methods,<sup>79</sup> can efficiently treat multiple protonation equilibrium, but require the use of a rigid structure. The complementarity of these two classes of methods prompted several attempts to devise methods explicitly treating both conformation and ionization changes, eventually leading to the development of constant-pH MD methods.<sup>80–90</sup> These methods allow protonable groups to periodically change their state during

Received: January 30, 2013

Revised: May 21, 2013

Published: May 22, 2013

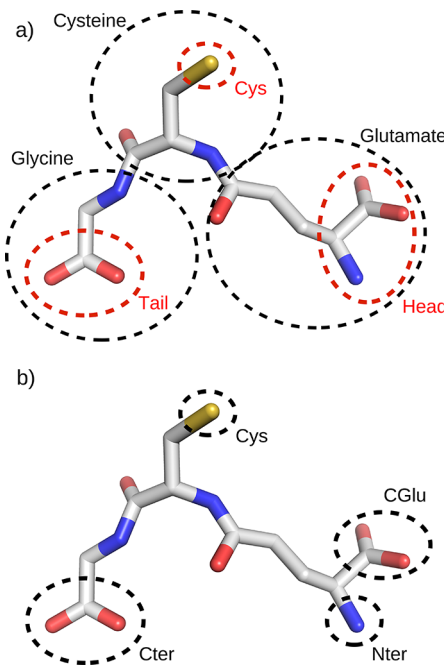


**Figure 1.** Glutathione molecule in reduced state (GSH). (a) Amino acid residues are marked in black dashed lines and the key groups for the conformational analysis are marked in red. (b) Titratable sites in GSH.

the simulation, thereby capturing the coupling between conformation and protonation.

The aim of this work is to perform a comprehensive conformational analysis of GSH and GSSG at different pH values. The constant-pH MD simulations sample both protonation and conformation and allow us to assign the key conformational transitions to the correct protonation microstate populations. It was also possible to obtain the different  $pK_a$  values of the two molecules and how their preferred conformations correlate with the structural constraints of several GSH binding proteins.

## ■ COMPUTATIONAL DETAILS AND METHODS

**Constant-pH MD Settings.** All simulations were performed using the stochastic titration constant-pH MD method implemented for the GROMACS package, developed by Baptista et al.<sup>80–82,91–94</sup> This method consists of a Molecular Mechanics (MM)/MD simulation in which the protonation states of the protein are periodically exchanged with new states obtained from a MC run using PB-derived free energy terms. The method relies on three blocks working in a stepwise approach. It starts with a PB/MC calculation to obtain a protonation state that is representative of both the solute conformation and the desired pH value. Next, a short MM/MD simulation ( $\tau_{rlx} = 0.2$  ps in this study) with the frozen solute is required to get the relaxation of the local water molecules. Finally, a production MM/MD simulation of the unconstrained system is performed ( $\tau_{prt} = 2.0$  ps in this study).

Both GSH and GSSG molecules were simulated at 24 pH values: from 0.5 to 12.0 in steps of 0.5. All carboxylic groups were titrated below pH 6.5, while the amino and thiol groups were titrated at pH 6.5 and above. It represents a total number of four titrating sites in GSH and six in GSSG. Three replicates of 100 ns were done for each pH value. A total number of 144 simulations were performed accounting for 14.4  $\mu$ s.

**MM/MD Settings.** The MM/MD simulations were performed using GROMACS 4.0.7<sup>95,96</sup> and the GROMOS96 54A7 force field.<sup>97</sup> The leapfrog algorithm was used with a 2 fs time step. The structures were solvated by 816 SPC<sup>98</sup> water molecules for GSH and 1135 for GSSG. A rhombic dodecahedral simulation box with periodic boundary conditions was used. The nonbonded interactions were treated using a twin-range cutoff of 8/14 Å and the neighbor lists were updated every 10 fs. Electrostatic long-range interactions were treated with a generalized reaction field<sup>99</sup> with a relative dielectric constant of 54<sup>100</sup> and an ionic strength of 0.1 M.<sup>81</sup> The Berendsen coupling<sup>101</sup> was used to treat temperature (310 K) and pressure (1 bar) with coupling constants of 0.1 and 0.5, respectively. Solvent and solute were separately coupled to the temperature bath. Isothermal compressibility of  $4.5 \times 10^{-5}$  bar<sup>-1</sup> was used. All bonds were constrained using the P-LINCS algorithm.<sup>102</sup>

The minimization procedure used a combination of steepest descent and limited-memory Broyden-Fletcher-Goldfarb-Shanno methods. The initiation was performed in 3 steps of 100 ps, 200 ps, and 200 ps with different restraints.

**PB/MC Settings.** The PB/MC calculations were done as previously described.<sup>79</sup> The MEAD 2.2.9<sup>103</sup> software package was used for PB calculations. The atomic charges and radii<sup>79</sup> were taken from the GROMOS96 54A7 force field. The model compound  $pK_a$  values used (7.46 for Nter, 4.62 for CGlu, 3.19 for Cter, and 8.58 for Cys) were obtained following a calibration method previously reported.<sup>104</sup> In the case of Cter and Cys, we repeated the procedure with constant-pH MD simulations of the pentapeptides and the GROMOS96 54A7 force field. For Nter and CGlu, we followed a slightly different approach with simulations of free amino acids (see Supporting Information for details). We used a dielectric constant of 2 for the protein and 80 for the solvent. Grid spacing of 0.25 and 1.0 Å were used in the finite difference focusing procedure.<sup>105</sup> The molecular surface was determined using a rolling probe of 1.4 Å and the Stern layer was 2 Å. The temperature used was 310 K and the ionic strength was 0.1 M.

The MC calculations were performed using the PETIT (version 1.5)<sup>106</sup> software with  $10^5$  steps for each calculation. Each step consisted of a cycle of random choices of protonation state (including tautomeric forms) for all individual sites and for pairs of sites with a coupling above 2.0  $pK_a$  units,<sup>106,107</sup> followed by the acceptance/rejection step according to Metropolis criterion.<sup>108</sup> The last protonation state is used for the MM/MD part.

**Analyses.** The last 90 ns of each simulation were used for analysis. Usually with small peptides the conformational properties converge very rapidly. However, due to the protonation/conformation coupling, the conformational space is only sampled correctly when the protonation has converged. At all pH values, the protonation converged well before the 10 ns discarded. Several tools from the GROMACS software package<sup>95,96</sup> were used and others were developed in-house. The PyMOL 0.99RC6 software (<http://www.pymol.org>) was used to obtain rendered conformational images.

Energy landscapes were obtained from different 2D spaces by computing kernel estimates of the data probability densities<sup>109</sup> on grids of  $(0.05 \text{ \AA})^2$  bins, using a Gaussian kernel. The probability density surface was then converted to an energy surface according to

$$E(\vec{x}) = -RT \ln \frac{P(\vec{x})}{P_{\max}}$$

where  $\vec{x}$  is a coordinate in a 2D space and  $P_{\max}$  is the maximum of the probability density function,  $P(\vec{x})$ .

The calculations of correlation-corrected errors for averages were computed using standard methods based on the autocorrelation function of the property measured to determine the number of independent blocks in the simulations.<sup>110</sup>

## RESULTS AND DISCUSSION

**Titration with Constant-pH MD.** The titration curves of GSH and GSSG (Figure 2) were computed by averaging at

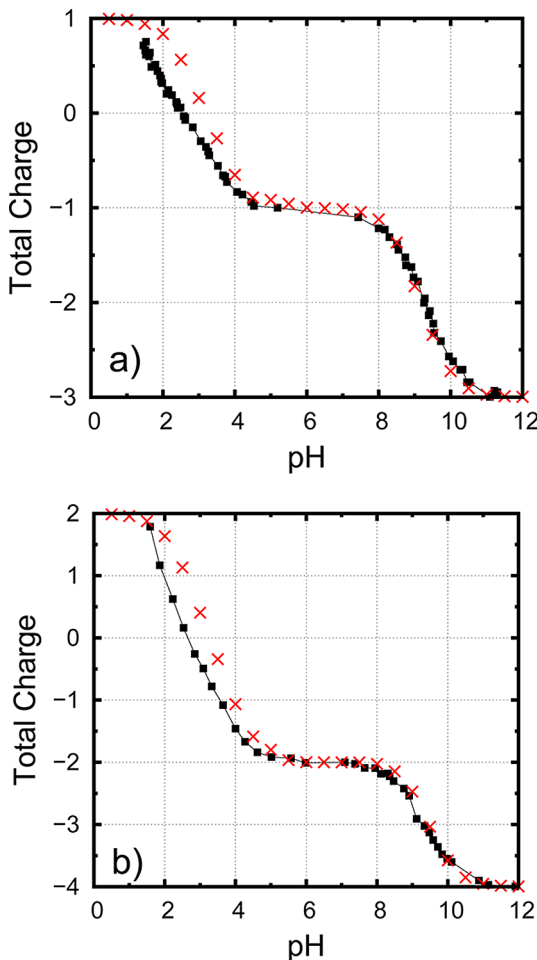


**Figure 2.** Titration curves of GSH (a) and GSSG (b) obtained from simulation (red crosses) and experiment (black squares).<sup>77</sup>

each pH value the occupancy of all titratable sites over 270 ns (discarding the initial 10 ns for each replicate). Both theoretical and experimental titration curves exhibit two transitions, one in the acidic and another in the basic region. In the case of GSH the first transition corresponds to the deprotonation of the two carboxylic groups (CGlu and Cter) and the second to the deprotonation of Cys residue and Nter. In the GSSG titration, the first transition corresponds to the deprotonation of the four carboxylic groups and the second to the deprotonation of the two Nter. Our results show a strong agreement with experiment (Figure 2), indicating that our method correctly samples the protonation of the various titratable sites in GSH and

GSSG. There are small deviations of the titration curves (more pronounced in the acidic region) which may be explained by a strong interaction of Nter with CGlu that, due to its electronic nature, becomes hard to model correctly using approximate methods without polarization. This poorly modeled interaction would in fact stabilize the ionized forms of the two groups involved and, consequently, lower the acid and increase the amine  $pK_a$  values. From the constant-pH MD simulations, we calculated the  $pK_a$  values of each titrable site and obtained 4 values for GSH and 3 for GSSG (Tables 1 and 2).

**Table 1.**  $pK_a$  Values Obtained for GSH in this Work and Different Experimental Studies

residue	predicted	ref 77	ref 111	ref 73	ref 76
CGlu	$2.69 \pm 0.01$	2.12		2.05	2.13
Cter	$3.68 \pm 0.04$	3.53	3.59	3.40	3.51
Cys	$8.88 \pm 0.01$	8.66	8.75	8.72	8.74
Nter	$9.46 \pm 0.01$	9.62	9.65	9.62	9.66

**Table 2.**  $pK_a$  Values Obtained for GSSG in This Work and Experiment

residue	predicted	ref 77 <sup>A</sup>	ref 112 <sup>A</sup>	ref 113 <sup>A</sup>
CGlu	$2.73 \pm 0.01$	2.3	2.09	1.96
Cter	$3.80 \pm 0.04$	3.7	3.49	3.50
Nter	$9.51 \pm 0.03$	9.2	9.18	9.18

<sup>A</sup>From the total titration curves, only one transition per site was observed, which resulted in only one  $pK_a$  value. The values were obtained by averaging both macroscopic  $pK_a$  values from experiments.

There is good agreement between our  $pK_a$  values and the experimental ones.<sup>73,76,77,111–113</sup> For some  $pK_a$  values the agreement is only qualitative but with errors within the method's predictive power.<sup>92,104</sup> As noted before, the difficulty in capturing the correct electrostatic environment of CGlu is reflected in its predicted  $pK_a$  shift of ~0.6 pK units for GSH. We should also note that the  $pK_a$  values calculated from the experimental curves are approximate due to a large overlap in the titration region of several sites (such as CGlu and Cter). Furthermore, an increase in one positive charge unit in the molecule does not correspond to a protonation of one group but to an average gain of a proton. When two groups are being titrated in the same pH region, it is not possible to obtain accurate  $pK_a$  values for those groups from the full titration curve. However, we also observed systematic shifts in the predicted  $pK_a$  values (all are overestimated excluding Nter in GSH), which suggests that some of these deviations may come from limitations in the model compound calibration procedure.

For GSSG, the average titration curves of the equivalent sites fit well to a Hill curve with small deviations from unity in the Hill coefficient values, suggesting noninteracting equivalent sites (see Supporting Information for individual titration curves). To quantify this, we calculated the  $\Delta pK_a$  values from a fit to a sum of two Henderson–Hasselbalch curves and obtained 0.63, 0.72, and 0.23 for CGlu, Cter, and Nter, respectively. Both values for the carboxylic acids are in agreement with experimental data (CGlu: 0.57<sup>112</sup> and 0.72;<sup>113</sup> Cter: 0.65<sup>112</sup> and 0.70<sup>113</sup>) and not far from the “statistical value” ( $\log 4 = 0.602$ ).<sup>114</sup> However, the value obtained for the Nter group is small compared with experiments (0.70<sup>112,113</sup>). This deviation to a lower value of  $\Delta pK_a$  indicates that the Nter group prefers to be protonated

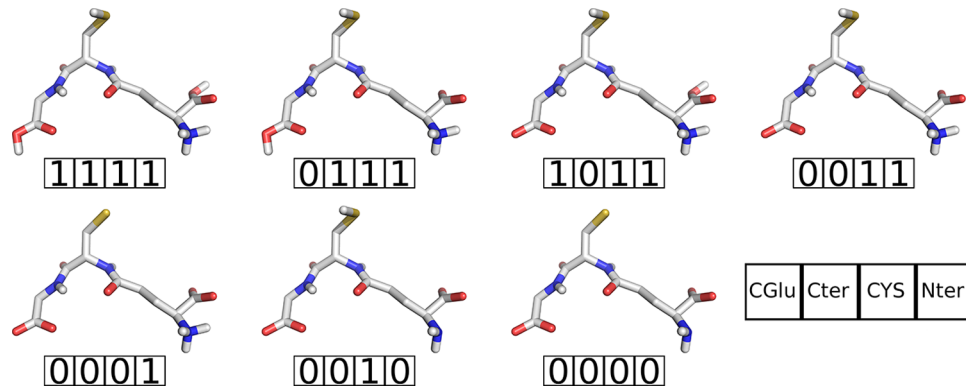


**Figure 3.** Seven major protonation states of GSH. (0) when it is deprotonated and (1) when it is protonated. The site sequence used goes from the lowest to the highest  $pK_a$  values.

when the equivalent site receives a proton. One possible explanation for this result is that both Nter groups in GSSG are overstabilizing each other in the neutral forms, which has been previously observed for primary amines in GROMOS force fields.<sup>81,83</sup>

The  $pK_a$  values of CGlu, Cter, and Nter groups are similar in GSH and GSSG. This indicates that a more complex structure of GSSG does not significantly change the environment of the titrable groups that could influence their  $pK_a$  values.

Rabenstein analyzed the fraction of several protonation states of GSH as a function of pH using the estimated  $pK_a$  values.<sup>73</sup> There are 16 possible protonation states but only 7 occur with a significant probability (Figure 3). We also computed the fraction of each of these 7 protonation states as a function of pH and compared with experiment (Figure 4). The general

the idea that our simulations can correctly sample the protonation states of GSH.

**Conformational Analysis of GSH.** As expected, neither GSH nor GSSG have a uniquely defined structure in solution. GSH showed a large conformational variability at all simulated pH values. Figure 5 shows the distributions of radius of

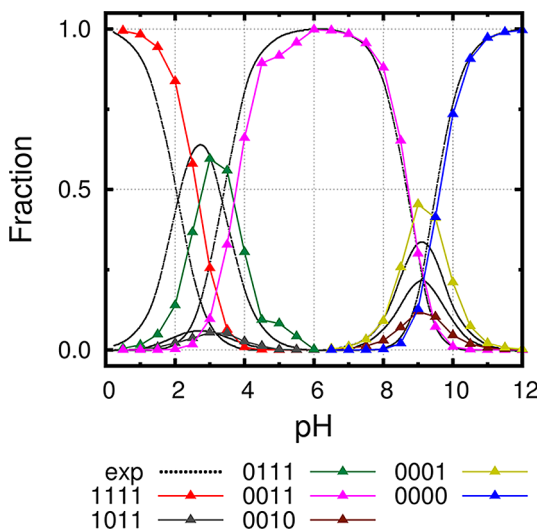


**Figure 4.** pH dependence of the fraction of the seven predominant protonation states in GSH. Experimental fractions were taken from ref 73.

agreement between experiment and simulation is very good and, as expected from the full titration curves and  $pK_a$  values, we observe a small deviation in the acidic region. Also, around pH 9.0 the two major populations present slightly different ratios. These differences originate mainly from the differences in the predicted individual  $pK_a$  values. Nevertheless, the predictive ability of these fractions is remarkable, reinforcing

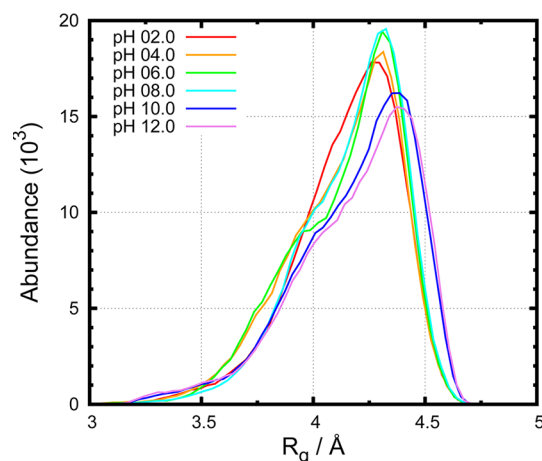


**Figure 5.** Radius of gyration ( $R_g$ ) histograms for GSH at different pH values. The curves for  $R_g$  at the pH values not shown are well behaved and respect the observed trend.

gyration ( $R_g$ ) at several pH values. The  $R_g$  values span a significant interval, with a shift toward larger radius. The distribution hardly varies with pH, but there is a slight increase at higher pH values meaning that the molecule samples more extended conformations upon deprotonation. In particular, the ionization of the two carboxylic groups generates a small repulsion, which is aggravated with the deprotonation of Cys. The deprotonation of Nter will have a similar effect due to the removal of a stabilizing positive charge.

Despite the information presented in Figure 5, it is clear that the  $R_g$  alone does not give enough detail at the molecular level to build a good conformational map for GSH. In fact, it can be advantageous to have more detailed measures like specific distances between key atoms. There are many possible distances that could be used but, in order to minimize redundancy, we simplified the problem to a few combinations. Figure 6a shows the histogram surface of the distance between the nitrogen atom in Nter and the closest oxygen atom in Cter (see Figure 1b) at different pH values. Interestingly, this

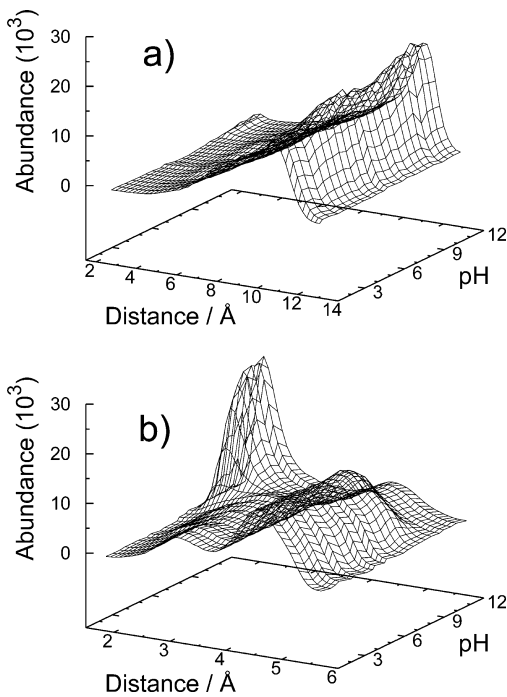


**Figure 6.** Histogram surface of two distances at different pH values. (a) Distance between the nitrogen atom of Nter and the closest oxygen atom of Cter; and (b) distance of sulfur atom in Cys and the hydrogen of the N–H group in Gly.

distance can capture similar structural variety obtained with  $R_g$ . Even though most conformations captured are extended, we were able to find closed structures with distances as low as 3 Å. Another key distance measured was between the sulfur atom of Cys and the hydrogen atom in the amide group of glycine (Figure 6b). In this case, we observed a significant pH dependent behavior. Below pH 9 large distances predominate, while above pH 9 the preferred distances are smaller (around 2.0 Å), indicating that the sulfur atom interacts with the main chain through hydrogen bonding. This strong interaction is favored upon deprotonation of the Cys residue ( $pK_a$  value of 8.88) when the thiolate becomes a reasonable hydrogen bond acceptor.

As mentioned above, there are many distances that capture in different ways the pH-dependent conformational behavior of GSH. We combined several of these distances in the characterization of the peptide conformational space (Figure 7). The Head to Tail (HT) distance (Figure 7a) was defined by the minimum distance between one of three atoms on the side we call Head (CGlu oxygens and Nter) and one of two atoms on the side we call Tail (Cter oxygens). The minimum distance between the sulfur atom and the five atoms on the Head and Tail sides (four oxygens and one nitrogen) results in the CYS-HT distance (Figure 7b). Combining these two special

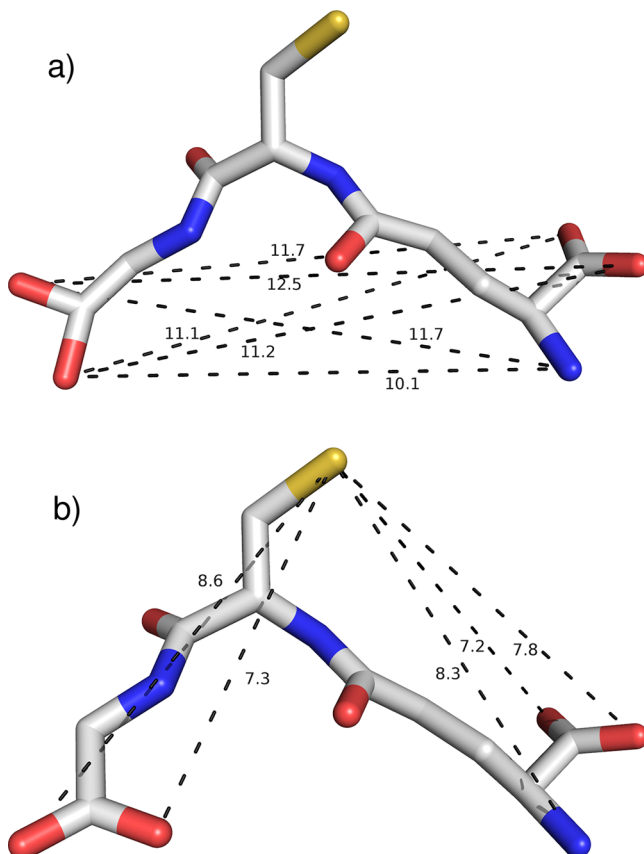


**Figure 7.** Representation of the distances selected to characterize the conformational space of GSH. (a) The Head to Tail distance (HT) is the shortest of these 6 distances. (b) The Cys to Head/Tail distance (CYS-HT) is the shortest of these 5 distances.

distances, we obtained a 2D-energy landscape at each pH value (Figure 8 and Supporting Information). In agreement with the  $R_g$  data, the predominant structures have a large HT distance typical of extended conformations. Nevertheless, there is a clear conformation dependence on pH. At low pH, three main regions are populated: one with large HT and CYS-HT distances; another with large HT and small CYS-HT; and finally, a region with medium HT and large CYS-HT (Figure 8a). From this distribution, we envisage completely extended structures, extended structures with small interactions involving the sulfur atom, and closed structures with a solvated sulfur atom. These observations reinforce the original idea that GSH has a very large conformational variability. As pH increases to neutrality, the landscapes maintain their global appearance (Figure 8b). This indicates that the deprotonation of the two carboxylic groups has only a small impact on the global conformation of GSH, as we noted from the  $R_g$  results (Figure 5). This observation agrees with the results from Kuchel and

**Table 3. Populations of Cysteine  $\chi_1^A$**

pH	a	ref 74	ref 67	b	ref 74 <sup>B</sup>	ref 67	c	ref 74 <sup>B</sup>	ref 67
07.0	0.31	0.33	0.12	0.33	0.33	0.33	0.37	0.33	0.53
09.0	0.35	0.31	0.43	0.39	0.48	0.28	0.26	0.21	0.27
12.0	0.43	0.29	0.33	0.45	0.50	0.49	0.13	0.21	0.16

<sup>A</sup>The three experimental data sets obtained from ref 74 were collected at pH 7, 9.1, and 12.4 (no experimental errors were reported). The authors in ref 67 infer pH by averaging over simulations at fixed protonation states. Rotamer a has the S atom *trans* to  $\alpha$ -H. Rotamer b has the S atom *trans* to NH group. Rotamer c has the S atom *trans* to CO group. <sup>B</sup>Rotamers b and c were assigned based on our results.

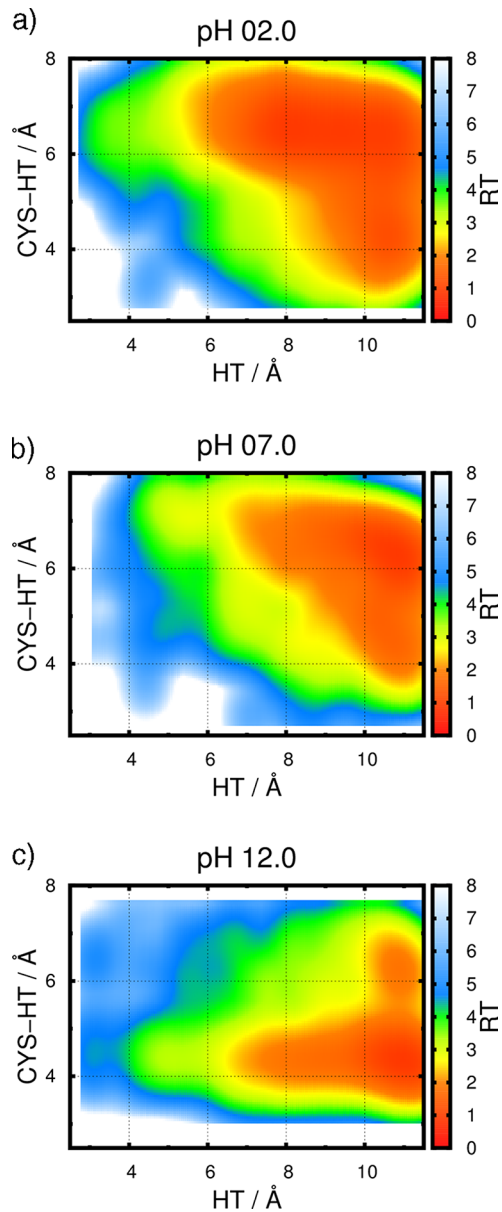


**Figure 8.** Free energy profiles for GSH at pH 2.0 (a), 7.0 (b), and 12.0 (c) using the selected distances as structural coordinates. HT refers to the distance between the atoms in the Head and Tail groups (see Figure 7a). CYS-HT refers to the shortest distance between the sulfur and the atoms in the Head and Tail groups (see Figure 7b).

co-workers who only observed a dynamic ensemble of rapidly interconverting conformations at acidic pH without any preferred structure.<sup>78</sup> However, for high pH values the landscape changes significantly (Figure 8c). The region with higher HT distances remains highly populated, but the one with large CYS-HT and smaller HT is gradually substituted by a new region with small HT and CYS-HT distances. This is characterized by more packed conformations with an ionized thiolate interacting through hydrogen bonding.

The deprotonation of the thiol in the cysteine residue seems to have an important role in GSH conformational space. It was experimentally observed that the  $\chi_1$  dihedral angle of cysteine has a pH dependent behavior (Table 3).<sup>74</sup> For pH values below 8.0 there are no preferable rotamers. However, above pH 8.0 there is a clear trend in the rotamer preferences. The authors

report the most abundant dihedral to be the one *trans* to the cysteine peptide nitrogen (*b*) or carbonyl group (*c*), indistinguishable from the NMR experiments.<sup>74</sup> The *a* rotamer is the one *trans* to the  $C_\alpha$  hydrogen and is reported to be less sensitive to pH changes.<sup>74</sup> From our simulations at pH 7.0, 9.0 and 12.0, we computed the populations of the  $\chi_1$  dihedral angles (Table 3), and unequivocally assigned the rotational isomer *b* as the most abundant. Also, the pH dependence behavior was well captured by our constant-pH MD simulations resulting in good agreement with experiment and with previous simulations reported by Rauk and co-workers (estimated from simulations at fixed protonation states).<sup>67</sup> Interestingly, these authors obtained a better prediction with all residues deprotonated (compared with pH 12.0). At this pH value, all residues are hardly titrating and, therefore, the differences between the two approaches have to be attributed to the simulation parameters. Figure 9 shows 90 structures at pH

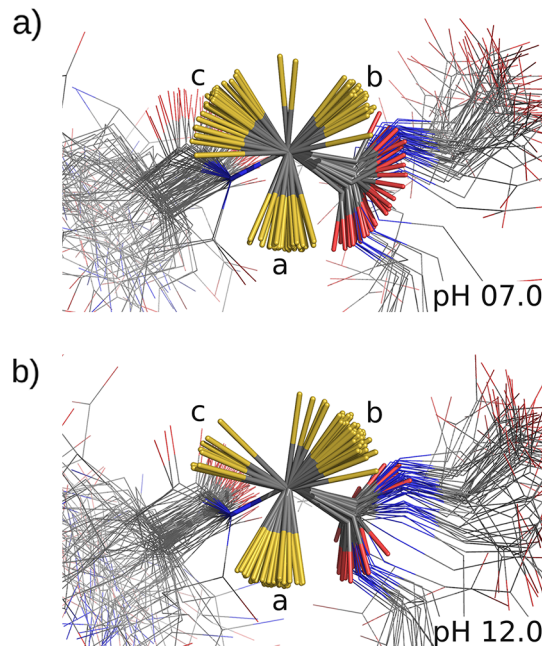


**Figure 9.** Superposition of 90 representative structures at pH 7 (a) and pH 12 (b) with N,  $C_\alpha$ , and  $C_\beta$  atoms fitted. The  $\chi_1$  rotational isomer regions are identified. All protons are omitted for clarity.

7.0 and 12.0 with the N,  $C_\alpha$  and  $C_\beta$  atoms from cysteine fitted. This figure illustrates the fact that there is no preferable rotamer at pH 7.0, while at pH 12.0 one rotamer becomes more abundant (*b*) and another is scarcely sampled (*c*).

**GSH Conformations in Protein Active Sites.** There are several protein structures in the Protein Data Bank (PDB, [www.pdb.org](http://www.pdb.org))<sup>115</sup> which contain GSH or GSSG.<sup>7–62</sup> From an initial data set, we removed all structures where GSH was chemically modified. We also discarded the structures without a clear description of the pH at which the data was collected. The remaining structures were separated in 3 groups, GSH-transferases (GST), GSH-reductases (GSR), and *others*, where glutaredoxins and all remaining structures are included. For the final data set, we determined both HT and CYS-HT distances and plotted them over the 2D-energy landscape (from Figure 8) originating Figure 10. The structures were also divided into 2 groups of different pH values, one below 6.0, which was plotted in the landscape obtained at pH 4.5, and another above

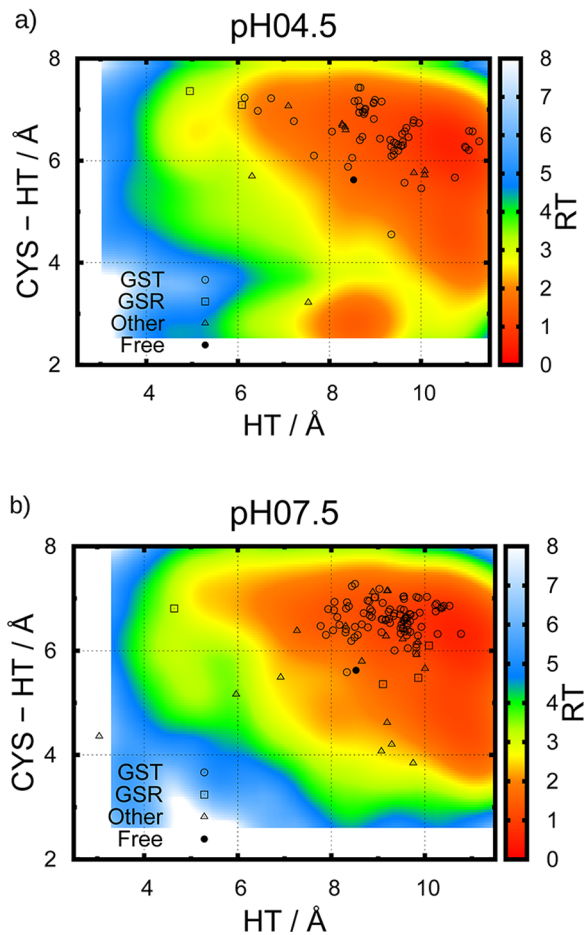


**Figure 10.** Energy landscapes obtained with the HT and CYS-HT distances at pH 4.5 (a) and 7.5 (b). The distances from crystal structures obtained with a pH lower than 6.0 were plotted in the pH 4.5 landscape, while the ones obtained with a pH higher than 6.0 were plotted on the pH 7.5 landscape. GST refers to glutathione transferases, GSR to glutathione reductases, other to more unusual proteins, and free refers to the Cambridge structure database<sup>116</sup> crystal structures.<sup>4–6</sup> The structures used were: 1B48,<sup>7</sup> 1EEM,<sup>8</sup> 1F3A,<sup>9</sup> 1JLV,<sup>10</sup> 1LBK,<sup>11</sup> 1OE7 and 1OE8,<sup>12</sup> 1U87,<sup>13</sup> 2FHE,<sup>14</sup> 2GDR,<sup>15</sup> 3FHS,<sup>16</sup> 3ISO,<sup>17</sup> 1PKW,<sup>18</sup> 1USB,<sup>19</sup> 2WJU,<sup>20</sup> 4ACS,<sup>21</sup> 1TDI,<sup>22</sup> 1R4W,<sup>23</sup> 3QAG,<sup>24</sup> 1MD3 and 1MD4,<sup>25</sup> 1ZGN,<sup>26</sup> 3CSI,<sup>27</sup> 6GSS,<sup>28</sup> 3CRT,<sup>29</sup> 3CRU and 3D0Z,<sup>29</sup> 2F8F, 2CA8 and 2CAQ,<sup>30</sup> 1XW6,<sup>31</sup> 1FW1,<sup>32</sup> 2JL4,<sup>33</sup> 2IMI,<sup>34</sup> 1IYH and 1IYI,<sup>35</sup> 1V40,<sup>36</sup> 2VCQ,<sup>37</sup> 2VCW,<sup>38</sup> 2VCX,<sup>39</sup> 2VCZ,<sup>40</sup> 2VD0 and 2VD1,<sup>37</sup> 2IMD, 2IME and 2IMF,<sup>38</sup> 3OB7,<sup>39</sup> 3C8E,<sup>40</sup> 2HQM,<sup>41</sup> 3DK4 and 3DK8,<sup>42</sup> 3H4K,<sup>43</sup> 2X8H and 2X99,<sup>44</sup> 2PBJ,<sup>45</sup> 2HGS,<sup>46</sup> 3B29,<sup>47</sup> 2ZK2,<sup>48</sup> 3BHJ,<sup>49</sup> 3C1S,<sup>50</sup> 3FZ9 and 3FZA,<sup>51</sup> 3L4N,<sup>52</sup> 1KCG,<sup>53</sup> 1Q8M,<sup>54</sup> 1QGJ,<sup>55</sup> 1Y1A,<sup>56</sup> 2R4V,<sup>57</sup> 3E73,<sup>58</sup> 3L9W,<sup>59</sup> 3LVW,<sup>60</sup> 3P8F and 3P8G,<sup>61</sup> 1GRA.<sup>62</sup>

6.0, which was plotted in the landscape obtained at pH 7.5. In the Cambridge structure database,<sup>116</sup> there are also three GSH structures, measured at normal pressure.<sup>4–6</sup> The molecular structures obtained from these crystals are almost identical; therefore, we plotted in both landscapes one single distance set with the name *free* (Figure 10). This Cambridge crystal structure was well sampled at both pH 4.5 and 7.5, which suggests that the crystal packing had little or no effect on altering the preferred solution conformations.

Most GSH conformations extracted from the PDB fall inside the ~2 RT regions of the landscapes. This indicates that most proteins in our data set bind GSH in an extended conformation similar to the low energy conformations observed in solution.

At lower pH values (Figure 10a) in the region between 2 and 4 RT, we find three structures, one GSR and two others. The GSR shows only one GSH molecule bound with a HT distance relatively short (PDB: 1GRA<sup>62</sup>). The function of GSR is to reduce one GSSG to two GSH molecules, so at least one monomer of GSSG must bind strongly in a restrained conformation allowing the thiolate attack to the S-S bond and free reduced GSH. The two *other* conformations were obtained from membrane receptors expressed in *Escherichia coli* and refolded in the presence of both GSH and GSSG. In both cases, the authors acknowledge GSH presence but dismiss any important role besides being the needed reducing agent.<sup>53,54</sup>

At higher pH values, most structures also fall inside the region below 2 RT (Figure 10b). There is one GSR structure in the region around 3 RT that presents a similarly strained conformation of an internalized monomer from GSSG (PDB: 3DK8<sup>42</sup>). The structure with HT distance of around 6 Å is a chloride intracellular channel and, according to the authors, has some structural similarities with GSTs, but most residues that are normally found to interact with GSH are replaced by nonconservative substitutions in this protein.<sup>57</sup> As a consequence, it does not bind GSH in the regular active site, keeping it at the surface, trapped between two crystal images which might have strongly influenced its conformation. A very unusual conformation was captured with an HT distance of 3 Å. The peculiar GST belongs to the membrane associated proteins in eicosanoid and GSH metabolism (Figure 11a).<sup>47</sup>

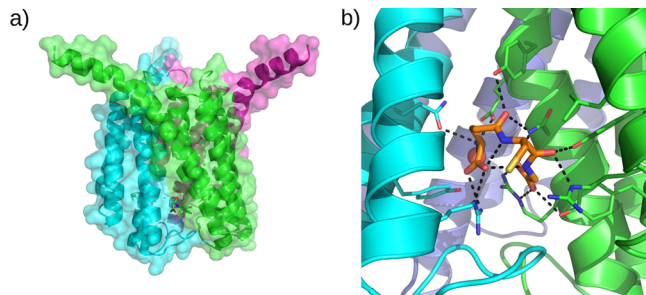


**Figure 11.** Structure of Leucotriene C4 synthase. Each monomer of the homotrimer was colored differently for clarity. Left panel (a) shows the secondary structure of the protein under a transparent surface and the GSH molecule (in sticks). Right panel (b) is focused on the GSH pocket showing electrostatic interactions (dashed line) between GSH (orange) and the protein.

The active enzyme is a homotrimer with very specific constraints concerning its GSH binding region. The tripeptide is internalized and stabilized through several hydrogen bonds and electrostatic interactions with several neighbor charged residues (Figure 11b). The charged microenvironment around GSH can induce highly distorted conformations completely inaccessible in water.

This conformational analysis helped us to identify how GSH is used in Nature. In general, GSH binds proteins at surface pockets and acts as a simple redox intermediate. From our data set, it appears that GSH prefers to associate with proteins in extended conformations. The outliers were easily identified with GSH acting as crystallization auxiliary or in very special proteins that hold it tightly for both structural and functional roles.

**Conformational Analysis of GSSG.** GSSG also presented a large conformational variability in solution at all simulated pH

values. Figure 12 shows the distributions of  $R_g$  at six pH values. Similarly to GSH, the GSSG  $R_g$  histograms also span a

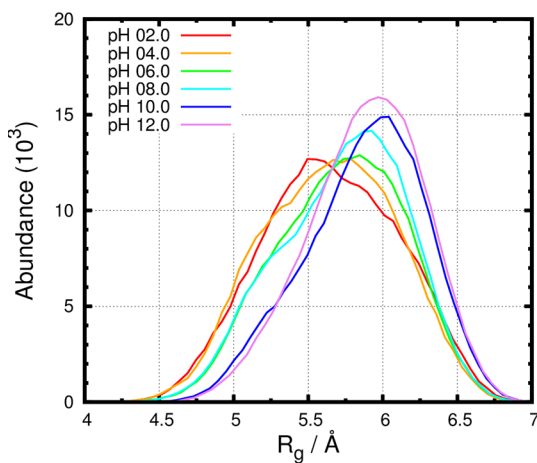


**Figure 12.** Radius of gyration ( $R_g$ ) histograms for GSSG at different pH values. The data for the remaining pH values respect the observed trend and were omitted for clarity.

significant interval with a clear trend of higher  $R_g$  as pH increases. The oxidation does not invert the anionic/cationic residue ratio; therefore, GSSG is also negatively charged at pH values above 4. Increasing pH will favor the more anionic species and induce internal repulsion resulting in higher  $R_g$  values. The histograms at pH 6–8 seem to exhibit a small bump at lower values of  $R_g$  but not significant enough to compare with the slightly bimodal behavior observed by Wu and co-workers.<sup>117</sup> The discrepancy might come from the different force fields used and/or the quantity of the conformational sampling.

As in the case of GSH, there are many possible interatomic distances that help to characterize the conformational behavior of GSSG. Figure 13 shows the distance distributions between the two nitrogen atoms in the Nter groups (Nter–Nter distance). From these histograms, there is a clear preference of GSSG for more extended structures, i.e., structures with large Nter–Nter distance. However, we observe a significant pH-

dependent behavior which, at low Nter–Nter distances (below 10 Å), is possible to interpret using direct interactions. At higher pH values (above 10.0) a Nter–Nter interaction will be unfavored due to the deprotonation of the Nter resulting in anionic head groups. Interestingly, at these pH values we captured conformations with very short distances that are typical of a direct hydrogen bond between the two amino groups, which can only be possible when at least one of them gets deprotonated. At intermediate pH values (between 4 and 8) there is a clear peak in the histogram formed with distances as low as 5 Å which are typical of zwitterionic head groups interacting via complementary charges (Nter and CGlu). At lower pH values (below 2) the histogram peak at short distances shifts toward larger distances (from ~5 to ~7 Å). This can be explained from the protonation of at least one CGlu group favoring a direct CGlu–CGlu hydrogen bond interaction slightly moving apart the Nter groups.

The analyses presented of the  $R_g$  and Nter–Nter distance in GSSG probably do not capture all the conformational space of the peptide and its dependence on pH. Nevertheless, it describes rather well the subtleties of a highly flexible molecule adapting to the different protonation states.

## CONCLUSIONS

In this work, we performed a full pH titration of GSH and GSSG, and a detailed study of the pH-dependent conformational space of these peptides.

The pH titration curves and the calculated  $pK_a$  values are in good agreement with experimental data,<sup>73,76,77,111</sup> indicating that our methodology is correctly sampling the protonation states of GSH and GSSG in solution. We also observed that the  $pK_a$  values for CGlu, Cter, and Nter groups are similar in oxidized and reduced glutathione which indicates that the oxidation does not introduce significant interactions shifting these values.

GSH proved to be a small peptide with a large conformational freedom without any clear structural preferences, which is in agreement with experiment.<sup>67,74,78,118</sup> Nevertheless, this conformational space was sensitive to changes in pH and we were able to identify the key features of this protonation/conformation coupling.

From the data set of GSH structures retrieved from the PDB server, we found that, in most proteins, GSH binds in the extended conformations also observed in solution. This cannot be dissociated from the fact that most structures are GSTs binding GSH transiently and, therefore, without the need to influence the peptide conformational preferences. The rare exceptions to these extended conformations happen in very unusual functional roles of GSH with the energetic compensation for the structural distortion coming from strong electrostatic interactions as in the case of leucotriene C4 synthase.<sup>47</sup>

GSSG also exhibited a large conformational variability at all simulated pH values. This was expected because its six residues arranged as a double tripeptide do not allow the formation of more complex structural elements. A small pH-dependence was also observed in the conformational space of this molecule but less evident than in GSH. Nevertheless, we clearly assigned several conformational transitions to (de)protonation events of key groups in GSSG.

Our results emphasize the usefulness of the stochastic titration constant-pH MD method<sup>80,81</sup> to simulate the conformational landscape of peptides and proteins with pH

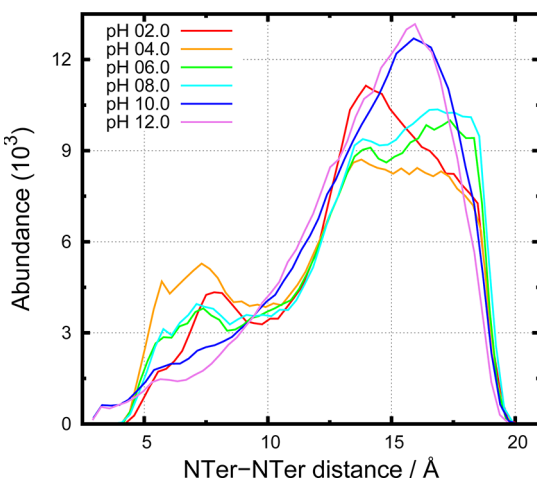


**Figure 13.** Distance histograms between nitrogen atoms of the two Nter groups. The data for the remaining pH values respect the observed trend and were omitted for clarity.

titrating sites. With this approach we obtained information on several conformational transitions associated with the protonation/conformation coupling which are usually inaccessible to classic MD simulations.

## ■ ASSOCIATED CONTENT

### S Supporting Information

Model compound calibration procedure. Titrations of the individual sites fitted to a Hill curve. Free energy profiles for GSH at all simulated pH values. This material is available free of charge via the Internet at <http://pubs.acs.org/>.

## ■ AUTHOR INFORMATION

### Corresponding Author

\*E-mail: machuque@fc.ul.pt. Phone: +351-21-7500112. Fax: +351-21-7500088.

### Notes

The authors declare no competing financial interest.

## ■ ACKNOWLEDGMENTS

We thank António M. Baptista and Maria José Calhorda for fruitful discussions and Sara R. R. Campos for the software to calculate free energy landscapes. We acknowledge financial support from Fundação para a Ciência e Tecnologia, through project PEst-OE/QUI/UI0612/2011 and grant SFRH/BD/81017/2011.

## ■ REFERENCES

- (1) Droege, W. *Physiol. Rev.* **2002**, *82*, 47–95.
- (2) Pastore, A.; Piemonte, F.; Locatelli, M.; Russo, A. L.; Gaeta, L. M.; Tozzi, G.; Federici, G. *Clin. Chem.* **2001**, *47*, 1467–1469.
- (3) Pastore, A.; Federici, G.; Bertini, E.; Piemonte, F. *Clin. Chim. Acta* **2003**, *333*, 19–39.
- (4) Wright, W. B. *Acta Crystallogr.* **1958**, *11*, 632–642.
- (5) Gorbitz, C. H. *Acta Chem. Scand. B* **1987**, *41*, 362–366.
- (6) Moggach, S. A.; Lennie, A. R.; Morrison, C. A.; Richardson, P.; Stefanowicz, F. A.; Warren, J. E. *CrystEngComm* **2010**, *12*, 2587–2595.
- (7) Xiao, B.; Singh, S. P.; Nanduri, B.; Awasthi, Y. C.; Zimniak, P.; Ji, X. *Biochemistry* **1999**, *38*, 11887–11894.
- (8) Board, P. G.; et al. *J. Biol. Chem.* **2000**, *275*, 24798–24806.
- (9) Gu, Y.; Singh, S. V.; Ji, X. *Biochemistry* **2000**, *39*, 12552–12557.
- (10) Oakley, A. J.; Harnnoi, T.; Udomsinprasert, R.; Jirajaroenrat, K.; Ketterman, A. J.; Wilce, M. C. J. *Protein Sci.* **2001**, *10*, 2176–2185.
- (11) Micaloni, C.; Kong, G. K. W.; Mazzetti, A. P.; Nuccetelli, M.; Antonini, G.; Stella, L.; McKinstry, W. J.; Polekhina, G.; Rossjohn, J.; Federici, G.; Ricci, G.; Parker, M. W.; Bello, M. L. *J. Mol. Biol.* **2003**, *325*, 111–122.
- (12) Johnson, K. A.; Angelucci, F.; Bellelli, A.; Hervé, M.; Fontaine, J.; Tsernoglou, D.; Capron, A.; Trottein, F.; Brunori, M. *Biochemistry* **2003**, *42*, 10084–10094.
- (13) Andújar-Sánchez, M.; Smith, A. W.; Clemente-Jimenez, J. M.; Rodriguez-Vico, F.; Las Heras-Vazquez, F. J.; Jara-Pérez, V.; Cámar-Artigas, A. *Biochemistry* **2005**, *44*, 1174–1183.
- (14) Rossjohn, J.; Feil, S. C.; Wilce, M. C. J.; Sexton, J. L.; Spithill, T. W.; Parker, M. W. *J. Mol. Biol.* **1997**, *273*, 857–872.
- (15) Tocheva, E. I.; Fortin, P. D.; Eltis, L. D.; Murphy, M. E. P. *J. Biol. Chem.* **2006**, *281*, 30933–30940.
- (16) Axarli, I.; Dhavala, P.; Papageorgiou, A.; Labrou, N. *Biochem. J.* **2009**, *422*, 247–256.
- (17) Han, Y. H.; Seo, H. A.; Kim, G. H.; Lee, C. K.; Kang, Y. K.; Ryu, K. H.; Chung, Y. J. *Protein Express. Purif.* **2010**, *73*, 74–77.
- (18) Grahn, E.; Novotny, M.; Jakobsson, E.; Gustafsson, A.; Grehn, L.; Olin, B.; Madsen, D.; Wahlberg, M.; Mannervik, B.; Kleywegt, G. J. *Acta Crystallogr., Sect. D* **2006**, *62*, 197–207.
- (19) Hederos, S.; Broo, K. S.; Jakobsson, E.; Kleywegt, G. J.; Mannervik, B.; Baltzer, L. *Proc. Natl. Acad. Sci. U.S.A.* **2004**, *101*, 13163–13167.
- (20) Tars, K.; Olin, B.; Mannervik, B. *J. Mol. Biol.* **2010**, *397*, 332–340.
- (21) Zhang, W.; Modén, O.; Tars, K.; Mannervik, B. *Chem. Biol.* **2012**, *19*, 414–421.
- (22) Gu, Y.; Guo, J.; Pal, A.; Pan, S. S.; Zimniak, P.; Singh, S. V.; Ji, X. *Biochemistry* **2004**, *43*, 15673–15679.
- (23) Ladner, J. E.; Parsons, J. F.; Rife, C. L.; Gilliland, G. L.; Armstrong, R. N. *Biochemistry* **2004**, *43*, 352–361.
- (24) Zhou, H.; Brock, J.; Liu, D.; Board, P. G.; Oakley, A. J. *J. Mol. Biol.* **2012**, *420*, 190–203.
- (25) Kong, G. K. W.; Polekhina, G.; McKinstry, W. J.; Parker, M. W.; Dragani, B.; Aceto, A.; Paludi, D.; Principe, D. R.; Mannervik, B.; Stenberg, G. *J. Biol. Chem.* **2003**, *278*, 1291–1302.
- (26) Cesareo, E.; Parker, L. J.; Pedersen, J. Z.; Nuccetelli, M.; Mazzetti, A. P.; Pastore, A.; Federici, G.; Caccuri, A. M.; Ricci, G.; Adams, J. J.; Parker, M. W.; Bello, M. L. *J. Biol. Chem.* **2005**, *280*, 42172–42180.
- (27) Parker, L. J.; Ciccone, S.; Italiano, L. C.; Primavera, A.; Oakley, A. J.; Morton, C. J.; Hancock, N. C.; Bello, M. L.; Parker, M. W. *J. Mol. Biol.* **2008**, *380*, 131–144.
- (28) Oakley, A. J.; Bello, M. L.; Battistoni, A.; Ricci, G.; Rossjohn, J.; Villar, H. O.; Parker, M. W. *J. Mol. Biol.* **1997**, *274*, 84–100.
- (29) Sagermann, M.; Chapleau, R. R.; DeLorimier, E.; Lei, M. *Protein Sci.* **2009**, *18*, 217–228.
- (30) Baiocco, P.; Gourlay, L. J.; Angelucci, F.; Fontaine, J.; Hervé, M.; Miele, A. E.; Trottein, F.; Brunori, M.; Bellelli, A. *J. Mol. Biol.* **2006**, *360*, 678–689.
- (31) Patskovsky, Y.; Patskovska, L.; Almo, S. C.; Listowsky, I. *Biochemistry* **2006**, *45*, 3852–3862.
- (32) Polekhina, G.; Philip, G.; Blackburn, A. C.; Parker, M. W. *Biochemistry* **2001**, *40*, 1567–1576.
- (33) Marsh, M.; Shoemark, D. K.; Jacob, A.; Robinson, C.; Cahill, B.; Zhou, N. Y.; Williams, P. A.; Hadfield, A. T. *J. Mol. Biol.* **2008**, *384*, 165–177.
- (34) Wang, Y.; Qiu, L.; Ranson, H.; Lumjuan, N.; Hemingway, J.; Setzer, W.; Meehan, E. J.; Chen, L. *J. Struct. Biol.* **2008**, *164*, 228–235.
- (35) Inoue, T.; Irikura, D.; Okazaki, N.; Kinugasa, S.; Matsumura, H.; Uodome, N.; Yamamoto, M.; Kumasaki, T.; Miyano, M.; Kai, Y.; Urade, Y. *Nat. Struct. Biol.* **2003**, *10*, 291–296.
- (36) Inoue, T.; Okano, Y.; Kado, Y.; Aritake, K.; Irikura, D.; Uodome, N.; Okazaki, N.; Kinugasa, S.; Shishitani, H.; Matsumura, H.; Kai, Y.; Urade, Y. *J. Biochem.* **2004**, *135*, 279–283.
- (37) Hohwy, M.; Spadola, L.; Lundquist, B.; Hawtin, P.; Dahmén, J.; Groth-Clausen, I.; Nilsson, E.; Persdotter, S.; von Wachenfeldt, K.; Folmer, R. H. A.; Edman, K. *J. Med. Chem.* **2008**, *51*, 2178–2186.
- (38) Thompson, L. C.; Ladner, J. E.; Codreanu, S. G.; Harp, J.; Gilliland, G. L.; Armstrong, R. N. *Biochemistry* **2007**, *46*, 6710–6722.
- (39) Gibson, L. M.; Celeste, L. R.; Lovelace, L. L.; Lebioda, L. *Acta Crystallogr., Sect. D* **2010**, *67*, 60–66.
- (40) Stourman, N. V.; Branch, M. C.; Schaab, M. R.; Harp, J. M.; Ladner, J. E.; Armstrong, R. N. *Biochemistry* **2011**, *50*, 1274–1281.
- (41) Yu, J.; Zhou, C. Z. *Proteins Struct. Funct. Bioinf.* **2007**, *68*, 972–979.
- (42) Berkholz, D. S.; Faber, H. R.; Sawides, S. N.; Karplus, P. A. *J. Mol. Biol.* **2008**, *382*, 371–384.
- (43) Angelucci, F.; Sayed, A. A.; Williams, D. L.; Boumis, G.; Brunori, M.; Dimastrogiovanni, D.; Miele, A. E.; Pauly, F.; Bellelli, A. *J. Biol. Chem.* **2009**, *284*, 28977–28985.
- (44) Angelucci, F.; Dimastrogiovanni, D.; Boumis, G.; Brunori, M.; Miele, A. E.; Saccoccia, F.; Bellelli, A. *J. Biol. Chem.* **2010**, *285*, 32557–32567.
- (45) Yamada, T.; Takusagawa, F. *Biochemistry* **2007**, *46*, 8414–8424.
- (46) Polekhina, G.; Board, P. G.; Gali, R. R.; Rossjohn, J.; Parker, M. W. *EMBO J.* **1999**, *18*, 3204–3213.
- (47) Saino, H.; Ago, H.; Ukita, Y.; Miyano, M. *Acta Crystallogr., Sect. F* **2011**, *67*, 1666–1673.

- (48) Waku, T.; Shiraki, T.; Oyama, T.; Fujimoto, Y.; Maebara, K.; Kamiya, N.; Jingami, H.; Morikawa, K. *J. Mol. Biol.* **2009**, *385*, 188–199.
- (49) Bateman, R. L.; Rauh, D.; Tavshanjian, B.; Shokat, K. M. *J. Biol. Chem.* **2008**, *283*, 35756–35762.
- (50) Yu, J.; Zhang, N. N.; Yin, P. D.; Cui, P. X.; Zhou, C. Z. *Proteins Struct. Funct. Bioinf.* **2008**, *72*, 1077–1083.
- (51) Couturier, J.; San Koh, C.; Zaffagnini, M.; Winger, A. M.; Gualberto, J. M.; Corbier, C.; Decottignies, P.; Jacquot, J. P.; Lemaire, S. D.; Didierjean, C.; Rouhier, N. *J. Biol. Chem.* **2009**, *284*, 9299–9310.
- (52) Luo, M.; Jiang, Y. L.; Ma, X. X.; Tang, Y. J.; He, Y. X.; Yu, J.; Zhang, R. G.; Chen, Y.; Zhou, C. Z. *J. Mol. Biol.* **2010**, *398*, 614–622.
- (53) Radaev, S.; Rostro, B.; Brooks, A. G.; Colonna, M.; Sun, P. D. *Immunity* **2001**, *15*, 1039–1049.
- (54) Radaev, S.; Kattah, M.; Rostro, B.; Colonna, M.; Sun, P. D. *Structure* **2003**, *11*, 1527–1535.
- (55) Mirza, O.; Henriksen, A.; Østergaard, L.; Welinder, K. G.; Gajhede, M. *Acta Crystallogr., Sect. D* **2000**, *56*, 372–375.
- (56) Blamey, C. J.; Ceccarelli, C.; Naik, U. P.; Bahnsen, B. J. *Protein Sci.* **2005**, *14*, 1214–1221.
- (57) Cromer, B. A.; Gorman, M. A.; Hansen, G.; Adams, J. J.; Coggan, M.; Littler, D.; Brown, L. J.; Mazzanti, M.; Breit, S. N.; Curmi, P. M. G.; Dulhunty, A. F.; Board, P. G.; Parker, M. W. *J. Mol. Biol.* **2007**, *374*, 719–731.
- (58) Zhang, W.; Wang, L.; Liu, Y.; Xu, J.; Zhu, G.; Cang, H.; Li, X.; Bartlam, M.; Hensley, K.; Li, G.; Rao, Z.; Zhang, X. C. *J. Mol. Biol.* **2009**, *23*, 1387–1392.
- (59) Roosild, T. P.; Castronovo, S.; Healy, J.; Miller, S.; Pliotas, C.; Rasmussen, T.; Bartlett, W.; Conway, S. J.; Booth, I. R. *Proc. Natl. Acad. Sci. U.S.A.* **2010**, *107*, 19784–19789.
- (60) Biterova, E. I.; Barycki, J. J. *J. Biol. Chem.* **2010**, *285*, 14459–14466.
- (61) Yuan, C.; Chen, L.; Meehan, E. J.; Daly, N.; Craik, D. J.; Huang, M.; Ngo, J. C. *BMC Struct. Biol.* **2011**, *11*, 30.
- (62) Karplus, P. A.; Schulz, G. E. *J. Mol. Biol.* **1989**, *210*, 163–180.
- (63) Rauk, A.; Armstrong, D. A.; Berges, J. *Can. J. Chem.* **2001**, *79*, 405–417.
- (64) Zamora, M. A.; Baldoni, H. A.; Rodriguez, A. M.; Enriz, R. D.; Sosa, C. P.; Perczel, A.; Kucsman, A.; Farkas, A.; Deretey, E.; Vank, J. C.; Csizmadia, I. G. *Can. J. Chem.* **2002**, *80*, 832–844.
- (65) Klipfel, M. W.; Zamora, M. A.; Rodriguez, A. M.; Fidanza, N. G.; Enriz, R. D.; Csizmadia, I. G. *J. Phys. Chem. A* **2003**, *107*, 5079–5091.
- (66) Klochkov, A. V.; Khairutdinov, B. I.; Tagirov, M. S.; Klochkov, V. V. *Magn. Reson. Chem.* **2005**, *43*, 948–951.
- (67) Lampela, O.; Juffer, A. H.; Rauk, A. *J. Phys. Chem. A* **2003**, *107*, 9208–9220.
- (68) Han, Y.; HaoMiao, Z.; Jian, S. *Sci. China Ser. B* **2007**, *50*, 660–664.
- (69) Dourado, D. F. A. R.; Fernandes, P. A.; Ramos, M. J. *J. Phys. Chem. B* **2010**, *114*, 12972–12980.
- (70) Dringen, R.; Koehler, Y.; Derr, L.; Tomba, G.; Schmidt, M. M.; Treccani, L.; Ciacchi, L. C.; Rezwan, K. *Langmuir* **2011**, *27*, 9449–9457.
- (71) Ding, V. Z. Y.; Dawson, S. S. H.; Lau, L. W. Y.; Lee, D. R.; Galant, N. J.; Setiadi, D. H.; Jojart, B.; Szori, M.; Mucsi, Z.; Viskolcz, B.; Jensen, S. J. K.; Csizmadia, I. G. *Chem. Phys. Lett.* **2011**, *507*, 168–173.
- (72) Fiser, B.; Szori, M.; Jojart, B.; Izsak, R.; Csizmadia, I. G.; Viskolcz, B. *J. Phys. Chem. B* **2011**, *115*, 11269–11277.
- (73) Rabenstein, D. L. *J. Am. Chem. Soc.* **1973**, *95*, 2797–2803.
- (74) Fujiwara, S.; Formicka-Kozlowska, G.; Kozlowski, H. *Bull. Chem. Soc. Jpn.* **1977**, *50*, 3131–3135.
- (75) Huckerby, T. N.; Tudor, A. J.; Dawber, J. G. *J. Chem. Soc., Perkin Trans. 2* **1985**, 759–763.
- (76) Krezel, A.; Bal, W. *Org. Biomol. Chem.* **2003**, *1*, 3885–3890.
- (77) Pirie, N. W.; Pinhey, K. G. *J. Biol. Chem.* **1929**, *84*, 321–333.
- (78) York, M. J.; Beilharz, G. R.; Kuchel, P. W. *Int. J. Pept. Protein Res.* **1987**, *29*, 638–646.
- (79) Teixeira, V. H.; Cunha, C. A.; Machuqueiro, M.; Oliveira, A. S. F.; Victor, B. L.; Soares, C. M.; Baptista, A. M. *J. Phys. Chem. B* **2005**, *109*, 14691–14706.
- (80) Baptista, A. M.; Teixeira, V. H.; Soares, C. M. *J. Chem. Phys.* **2002**, *117*, 4184–4200.
- (81) Machuqueiro, M.; Baptista, A. M. *J. Phys. Chem. B* **2006**, *110*, 2927–2933.
- (82) Machuqueiro, M.; Baptista, A. M. *J. Am. Chem. Soc.* **2009**, *131*, 12586–12594.
- (83) Börjesson, U.; Hünenberger, P. H. *J. Chem. Phys.* **2001**, *114*, 9706.
- (84) Burgi, R.; Kollman, P. A.; van Gunsteren, W. F. *Proteins Struct. Funct. Bioinf.* **2002**, *47*, 469–480.
- (85) Lee, M. S.; Salsbury, F. R.; Brooks, C. L. *Proteins Struct. Funct. Bioinf.* **2004**, *56*, 738.
- (86) Mongan, J.; Case, D. A.; McCammon, J. A. *J. Comput. Chem.* **2004**, *25*, 2038.
- (87) Dlugosz, M.; Antosiewicz, J. M. *Chem. Phys.* **2004**, *302*, 161–170.
- (88) Dlugosz, M.; Antosiewicz, J. M.; Robertson, A. D. *Phys. Rev. E* **2004**, *69*, 021915.
- (89) Stern, H. A. *J. Chem. Phys.* **2007**, *126*, 164112.
- (90) Vorobjev, Y. N. *J. Comput. Chem.* **2012**, *33*, 832–842.
- (91) Machuqueiro, M.; Baptista, A. M. *Biophys. J.* **2007**, *92*, 1836–1845.
- (92) Machuqueiro, M.; Baptista, A. M. *Proteins Struct. Funct. Bioinf.* **2008**, *72*, 289–298.
- (93) Campos, S. R. R.; Baptista, A. M. *J. Phys. Chem. B* **2009**, *113*, 15989–16001.
- (94) Campos, S. R. R.; Machuqueiro, M.; Baptista, A. M. *J. Phys. Chem. B* **2010**, *114*, 12692–12700.
- (95) Berendsen, H. J. C.; van der Spoel, D.; van Drunen, R. *Comput. Phys. Commun.* **1995**, *91*, 43–56.
- (96) Hess, B.; Kutzner, C.; Van Der Spoel, D.; Lindahl, E. *J. Chem. Theory Comput.* **2008**, *4*, 435–447.
- (97) Schmid, N.; Eichenberger, A. P.; Choutko, A.; Riniker, S.; Winger, M.; Mark, A. E.; Van Gunsteren, W. F. *Eur. Biophys. J.* **2011**, *1*–14.
- (98) Hermans, J.; Berendsen, H. J. C.; van Gunsteren, W. F.; Postma, J. P. M. *Biopolymers* **1984**, *23*, 1513–1518.
- (99) Tironi, I. G.; Sperb, R.; Smith, P. E.; van Gunsteren, W. F. *J. Chem. Phys.* **1995**, *102*, 5451–5459.
- (100) Smith, P. E.; van Gunsteren, W. F. *J. Chem. Phys.* **1994**, *100*, 3169–3174.
- (101) Berendsen, H. J. C.; Postma, J. P. M.; van Gunsteren, W. F.; DiNola, A.; Haak, J. R. *J. Chem. Phys.* **1984**, *81*, 3684–3690.
- (102) Hess, B. *J. Chem. Theory Comput.* **2008**, *4*, 116–122.
- (103) Bashford, D.; Gerwert, K. *J. Mol. Biol.* **1992**, *224*, 473–486.
- (104) Machuqueiro, M.; Baptista, A. M. *Proteins Struct. Funct. Bioinf.* **2011**, *79*, 3437–3447.
- (105) Gilson, M. K.; Sharp, K. A.; Honig, B. H. *J. Comput. Chem.* **1987**, *9*, 327–335.
- (106) Baptista, A. M.; Soares, C. M. *J. Phys. Chem. B* **2001**, *105*, 293–309.
- (107) Baptista, A. M.; Martel, P. J.; Soares, C. M. *Biophys. J.* **1999**, *76*, 2978–2998.
- (108) Metropolis, N.; Rosenbluth, A. W.; Rosenbluth, M. N.; Teller, A. H.; Teller, E. *J. Chem. Phys.* **1953**, *21*, 1087–1092.
- (109) Silverman, B. W. *Density estimation for statistics and data analysis*; Chapman and Hall: London, 1986.
- (110) Allen, P. M.; Tildesley, D. J. *Computer Simulation of Liquids*; Clarendon: Oxford, 1997.
- (111) Li, N. C.; Gawron, O.; Bascuas, G. *J. Am. Chem. Soc.* **1954**, *76*, 225–229.
- (112) Kozlowski, H.; Urbanska, J.; Sovago, I.; Varnagy, K.; Kiss, A.; Psychala, J.; Cherifi, K. *Polyhedron* **1990**, *9*, 831–837.
- (113) Noszál, B.; Szakács, Z. *J. Phys. Chem. B* **2003**, *107*, 5074–5080.
- (114) Noszál, B. *J. Phys. Chem.* **1986**, *90*, 4104–4110.

- (115) Berman, H. M.; Westbrook, J.; Feng, Z.; Gilliland, G.; Bhat, T. N.; Weissig, H.; Shindyalov, I. N.; Bourne, P. E. *Nucleic Acids Res.* **2000**, *28*, 235–242.
- (116) Allen, F. H. *Acta Crystallogr., Sect. B* **2002**, *58*, 380–388.
- (117) Zhang, R.; Zeng, W.; Meng, X.; Huang, J.; Wu, W. *Chem. Phys.* **2012**, *402*, 130–135.
- (118) Laurence, P. R.; Thomson, C. *Theor. Chim. Acta* **1980**, *57*, 25–41.